0026-895X/94/010065-09$03.00/0
Copyright © by The American Society for Pharmacology and Experimental Therapeutics
All rights of reproduction in any form reserved.
MOLECULAR PHARMACOLOGY, 45:65-73

MOL PHARM

Continuous Spectrofluorometric Analysis of Formyl Peptide Receptor Ternary Complex Interactions

RICHARD G. POSNER, SHAWN P. FAY, MARK D. DOMALEWSKI, and LARRY A. SKLAR

Cancer Center, Departments of Pathology and Cytometry, University of New Mexico School of Medicine, Albuquerque, New Mexico 87131 (S.P.F., M.D.D.), and National Flow Cytometry Resource M888, Los Alamos National Laboratory, Los Alamos, New Mexico 87545 (R.G.P., L.A.S.)

Received May 21, 1993; Accepted October 12, 1993

SUMMARY

Fluorescent formyl peptides have made it possible to study ligand-receptor-G protein (ternary complex) dynamics in real-time, but limitations to sample mixing and delivery in flow cytometry have interfered with continuous observation. We have taken advantage of the quenching of a fluoresceinated *N*-formyl pentapeptide upon binding to its receptor on permeabilized neutrophils to extend the analysis of the ternary complex dynamics to the second time scale. The association and dissociation of ligand in the presence and absence of saturating concentrations of GTP[S] were examined continuously and the results were found to be in agreement with results predicted previously from flow cytometry. We observe comparable initial rates for the formation of ligand-receptor (LR) binary complexes and ligand-receptor guanine nucleotide binding protein (LRG) ternary complexes, dissociation rates differing by two orders of magnitude, and slow interconversions between LR and LRG in the absence of guanine nucleotide. When fit by the ternary complex model, at least three sides of the model are required and the fit is improved if a significant fraction of receptors (RG) are allowed to be precoupled to G protein. One of the limitations of the analysis is that data fits are insensitive to additional parameters in the calculation which would permit analysis of all four sides of the ternary complex model. Experiments performed with subsaturating GTP[S] identified coexisting classes of LR and LRG and allowed analysis of the altered distribution between coupled and uncoupled receptors. At saturating nucleotide levels, the binding of GTP[S] and the breakup of the ternary complex occur on a subsecond time frame. This result is consistent with the idea that inside a neutrophil where GTP levels are several hundred μM, once ternary complex forms, ternary complex decomposition is rapid. Taken together, the observed rapid assembly and disassembly of ternary complex account for subsecond cell responses to ligand.

The binding of ligands to cell surface receptors initiates signals for cell activation. In neutrophils, cellular activation occurs via a sequence of interactions among chemoattractant ligand-receptor complexes and guanine nucleotide-binding proteins and cell responses are detected within seconds of exposure to the ligand (1). Evidence from several cell types suggest that in G protein-containing systems, there are at least three distinct ligand-receptor complexes (2–5) which we refer to in the neutrophil as LR, LRG, and LRX (a desensitized form of the receptor whose formation may be dependent upon phosphorylation; 6, 7). While radioligand techniques have been used to study the interactions of ligands, receptors, and G proteins (8, 9), the time resolution of the assays is limited to filtration times. Data in these systems are analyzed by a ternary complex formalism (10) shown in Fig. 1 as a cycle of stepwise interactions between L, R, and G. Limitations of the formalism, such as undefined stoichiometry of the components, have been pointed out (11). Because the dissociation rate constant for LR is often 0.1/sec, direct measurement of LR in radioligand assays may be impractical. In some systems it has only been possible to study LR dynamics in competitive assays in which a high affinity radiolabeled receptor antagonist is employed.

Recently we employed flow cytometry to examine L, R, and G interactions in permeabilized neutrophils (12). Flow cytometry intrinsically resolves free from bound ligand and the use of permeabilized neutrophils permits the detection of LRG and LR states (5). Equilibrium binding studies performed by cytometry indicated that the affinity of LRG for ligand is about two orders of magnitude greater than that of LR. In the absence of guanine nucleotide, a second class of receptors with affinity characteristics similar to LR was detected (12). This suggests that some fraction of LR sites remains uncoupled from G in the absence of guanine nucleotide or couple slowly, as has been indicated in other systems (13, 14). The kinetic studies performed by cytometry (12) revealed that the differences in affinity between LRG and LR were due primarily to differences in the dissociation rate constants (~1–2 × 10^{-3} sec^{-1} and ~10^{-1}

This work was supported at University of New Mexico School of Medicine by NIH Grant AI19032 and the University of New Mexico Cancer Center and at Los Alamos National Laboratory by RR 01315 and LDRD X195.

ABBREVIATIONS: GTP[S], guanosine 5′-*O*-(3-thiotriphosphate); tbocFLFLF, *tert*-butyloxycarbonyl-Phe-Leu-Phe-Leu-Phe; 5PEP, CHO-Met-Leu-Phe-Phe-Lys-fluorescein; LR, ligand-receptor; G, guanine nucleotide binding protein.

MOLECULAR PHARMACOLOGY
aspet
Downloaded from molpharm.aspetjournals.org at Thammasart University on December 2, 2012

MOL PHARM

MOLECULAR PHARMACOLOGY

sec^{-1}, respectively), while the association rate constants for LRG and LR (~2–3 × 10^7 sec^{-1} M^{-1}) were statistically indistinguishable. When the kinetic data for ligand binding to receptor were fit, large systematic errors were observed when simple one- or two-step models were used to analyze the data. The simplest model consistent with the data required at least three sides of the ternary complex model (Fig. 1) because fits using only sides 1 and 2 or sides 1 and 3 returned dissociation rates inconsistent with direct measurements and large systematic errors. The fits were improved by allowing the fraction of R and RG to be parameters (12). Sample delivery limitations made it impractical to measure association and dissociation kinetics with the same sample and limited the information about forward steps and rapid transitions.

In this study, we have described a new fluorimetric method that takes advantage of quenching via protonation in the receptor-binding pocket (15) to study the binding of a fluoresceinated pentapeptide (5PEP) to its receptor on permeabilized human neutrophils. The specifity of the ligand-receptor interaction is high and nonspecific interaction of the ligand with the membrane at nM ligand concentrations is not detectable (16). Whereas flow cytometry was limited by the sample delivery time of 5 sec, cuvette analysis allows for sample delivery and mixing within ~1 sec but requires an order of magnitude-increased cell density. The quenching provides better signal to noise than fluorescence polarization (17) and, unlike the methods using fluorescein antibodies (5, 6, 18), it allows measurement of both the forward and reverse steps in ligand binding. With stopped-flow mixing, resolution to 100 msec can be achieved (19). Here, we use the continuous cuvette methods to confirm and extend the flow cytometric analysis.

TERNARY COMPLEX MODEL

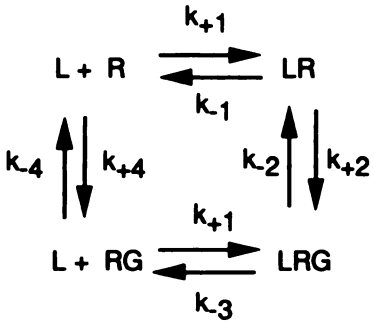

Fig. 1. The ternary complex formalism. Four sides of the ternary complex model are shown. The rate constant represent: k_{+1} and k_{-1}, the forward and reverse constant for binary complex formation; k_{+2} and k_{-2} the forward and reverse rate constant for ternary complex formation from LR and G; k_{+3} and k_{-3}, the forward and reverse rate constant for the formation of ternary complex from L and precoupled RG. k_{+4} and k_{-4} refer to coupling and upcoupling of R and G in the absence of ligand. In our analysis we have been unable to determine values for $k_{\pm4}$, and these two parameters have been set equal to 0. This model has five species (L, R, LRG, RG, and R) and two conservation laws. It thus requires three sets of differential equations to fully descibe the system. The differential equations that describe this model are:

$$d[LR]/dt = k_{+1}[L][R] - k_{-1}[LR] - k_{+2}[LR] + k_{-2}[LRG]$$

$$d[LRG]/dt = k_{+2}[LR] - k_{-2}[LRG] - k_{-3}[LRG] + k_{+1}[L][RG]$$

$$d[RG]/dt = k_{-3}[LRG] - k_{+1}[L][RG] + k_{+4}[R] - k_{-4}[RG]$$

The conservation laws are:

$$R = R_T - [LR] - [LRG] - [RG]$$

$$L = L_T - [LR] - [LRG]$$

where R_T and L_T are the total receptor and ligand concentrations. Note that this formalism does not involve nucleotide and that [G] is included implicitly in k_{+2} and k_{+4} (in which case it assumed that G ≫ R). It is not necessary to assume that L is in excess as the conservation laws account for changes in L.

Materials and Methods

Neutrophils and permeabilized neutrophils. Human neutrophils were prepared by the elutriation method of Tolley *et al.* (20) and permeabilized as described previously (5, 21). Briefly, stock solutions of digitonin (1 mg/ml in the intracellular buffer described below) were prepared daily. Neutrophils were suspended at 2 × 10^7/ml in the same buffer and incubated for 30 min at 37° with 15 μg/ml digitonin. Permeabilization was confirmed by the ability of guanine nucleotide to release bound fluorescent ligand (see below). In general, cell preparations were discarded when more than ~15% of the receptors were insensitive to guanine nucleotide, indicative of incomplete permeabilization. Alkylation of the permeabilized cells was accomplished by treating the cells with *N*-ethylmalemide at a concentration of 0.1 mM for 10 min at 37°.

Reagents. The pentapeptide 5PEP, a gift from Dr. Richard Freer, was prepared by the rapid mixed anhydride procedure (22), as described in detail by Sklar *et al.* (16). The polyclonal antibody to fluorescein was prepared (18) and its high affinity binding quantitated as described previously (23). The formyl peptide antagonist tboc-phe-leu-phe-leu-phe was obtained from Vega Biochemicals (Tucson, AZ). GTP[S] was obtained from Sigma (St. Louis, MO). Fluorescent beads used as calibration standards were obtained from Flow Cytometry Standards Corp. (Research Triangle, NC).

Buffers. The intracellular buffer described by Smolen *et al.* (21) (100 mM KCl, 20 mM NaCl, 1 mM EGTA, and 30 mM Hepes; pH 7.3) was supplemented with 0.1% bovine serum albumin, and 1 mM phenylmethylsulfonyl fluoride to stabilize the peptide fluorescence and 5 mM $MgCl_2$. We refer to this buffer as intracellular binding buffer. In earlier studies we used an extracellular buffer (30 mM Hepes, pH 7.0, 110 mM NaCl, 10 mM KCl, 1 mM $MgCl_2$, and 10 mM glucose with 0.1% bovine serum albumin to stabilize the peptide against hydrophopic interaction with the cuvettes and transfer pipettes) as a dilution buffer when transferring reagents.

Fluorescence measurements. Fluorescence was examined in photon-counting mode in an SLM-Aminco 8000 or 8000C spectrofluorometer (Urbana, IL) outfitted with a cylindrical cuvette adapter (16), cylindrical glass cuvette (Sienco, Morrison, CO), and a 2 × 5-mm stirbar (Bel-Art, Pequannock, NJ). The excitation was 490 nm and stray light was reduced with a 490 nm, 10 nm bandpass interference filter (Corion, Holliston, MA). The emission signal was monitored through a 520 nm, 10 nm bandpass interference filter (Corion) and a 3–70 OG Corning glass filter (Kopp, Pittsburgh, PA).

Calibration of fluorescent peptides. The concentrations of peptide solutions were determined as in Fay *et al.* (12). Briefly, we used fluorescent bead standards (Flow Cytometry Standards Corp.) that were quantitated according to peptide fluorescein equivalents per particle. Based on 2.33 × 10^6 particles/ml and 2.3 × 10^6 equivalents per bead, the fluorescein equivalent concentration was calculated to be 8.78 nM (12). The peptide fluorescence was determined to be 0.8 fluorescein equivalents per fluorescein 5′isothiocyanate-peptide. Typically, 1 nM free peptide provided ~25,000 photons per half-second interval.

Analysis of fractional receptor occupancy and quenching upon binding. Permeabilized cells were suspended at 10^7/ml in intracellular binding buffer (pH 7.3) and 200-μl aliquots were placed in the stirred cylindrical cuvette of an SLM 8000 or 8000C. The fluorescence was monitored continuously after the addition of fluorescent peptide

Downloaded from molpharm.aspetjournals.org at Thammasart University on December 2, 2012

MOL PHARM

MOLECULAR PHARMACOLOGY

(Fig. 2). The antibody to fluorescein is used in the evaluation of the relative intensities of the free and the bound ligand, as well as the mole fraction of the bound ligand. As illustrated in Fig. 2A, when excess nonfluorescent ligand is added before the addition of 5PEP, the relative fluorescence of the free ligand is given by A. Antibody binds and quenches the free fluorescent peptide within 1 sec at a rate constant of $\sim 10^8$ M^{-1} sec^{-1}. The addition of antibody to fluorescein quenches the fluorescence of the free 5PEP rapidly to D. In contrast, antibody fails to recognizes the receptor-bound pentapeptides. Upon binding to the receptor, the fluorescence of the 5PEP is partially quenched (B). Upon the addition of antibody to fluorescein, the fluorescence of the free peptide is rapidly quenched (C) while the fluorescein on the receptor bound peptides is protected in the binding pocket of the cell surface receptor (16). The fluorescence values A, B, C, and D can be related to the mole fractions of the fluorescent bound ligand according to the following scheme. I_f is the intensity of the free peptide, I_b is the intensity of the cell-bound peptide, I_a is the intensity of antibody-bound peptide, and X_b is the mole fraction of cell-bound peptide. Then A represents free ligand with intensity I_f; B represents a combination of free ligand and quenched bound ligand where the intensity is given by $I_f(1 - X_b) + I_bX_b$; C represents a combination of receptor-bound ligand and antibody-bound ligand, the intensity given by $I_bX_b + I_a(1 - X_b)$; and D represents the ligand bound to antibody where the intensity is I_a. Rearranging gives the residual fluorescence of the bound ligand $I_b/I_f = [(B - A)(A - D)/A(A - B + C - D)] + 1$, and the mole fraction bound $X_b = 1 - [(B - C)/(A - D)]$ (12, 16). The mole fraction of ligand bound at any point (f) along curve (indicated as "bound" in Fig. 2A) is given by $X_b(t) = [(A - f)/(A - B)][1 - (B - C)/(A - D)]$. Thus if the concentration of ligand total is (L_T), the concentration of bound ligand as a function of time is simply $X_b(t)[L_T]$.

Kinetic fluorometric analysis of ligand binding. Kinetic measurements of ligand binding to the neutrophil formyl peptide receptor using spectrofluorometric techniques were performed using the quenching that accompanies the binding of 5PEP (16) as a means to determine the amount of ligand bound as a function of time. Cell suspensions, equilibrated at 37°, were exposed to a calibrated solution of peptide (2 μl peptide to 200 μl 10^7 cells/ml). Binding data were acquired at 1-sec intervals on an SLM 8000 spectrofluorometer with a sample compartment modified to permit use of small volumes and facilitate rapid mixing. Individual concentrations of ligand were repeated in duplicate or triplicate in the presence and absence of varying concentrations of guanine nucleotide (as required by the experiment). Typically three concentrations of ligand were tested in a single experiment. Kinetic measurements of the dissociation of bound ligand from its receptor were performed by the addition of a large excess (2×10^{-5} M) of antagonist (tbocFLFLF). The absence of appreciable nonspecific binding was verified by two independent methods. The first involved a quantitative comparison of nonbinding ("blocked") samples in which cells were present (Fig. 2A, solid line) or absent; the second involved quantitative recovery of the peptide from the supernatant of nonbinding (blocked) cell suspensions.

Concentrations of fluorescent peptides were measured daily by comparison to the fluorescence of beads suspended at nominal concentrations ~1 nM. The concentration of free ligand and the ratio of the relative fluorescence of bound ligand to that of free ligand in solution were determined by the antibody to fluorescein and quenching as described above (12, 18). In most experiments, dilutions of 1% each were required during addition of GTP[S] and tbocFLFLF. Under conditions in which the net quenching upon binding is 20–30% of the total intensity, the dilution effect contributes to an apparent irreversibility in binding representing 6–10% of the bound ligand. This irreversible component was not corrected for in the data but was included as a parameter in the data analysis. Ligand concentrations are measured directly and are estimated to be reliable to ~10%; the determination of the LR concentration depends upon the value of quenching at pH 7.0 (~0.5), which is estimated to be reliable to ~10%.

Analysis of kinetic binding data. We analyzed kinetic experiments performed in the presence or absence of guanine nucleotide according to models related to the ternary complex (12). The best fits of the data were obtained when rate constants for three sides of the complete ternary complex model were used and the proportion of R and RG was allowed to vary. The coupled differential equations which describe ligand binding (Fig. 1) were solved numerically by Gears' method using the Los Alamos National Mathematics Library routine SDRVB. Parameter estimates were obtained using the International Mathematics and Statistics Library routine ZXSSQ based on the finite difference Levenberg-Marquardt algorithm for solving nonlinear least squares problems. The analysis was performed on a Cray YMP supercomputer at Los Alamos National Laboratory.

The modeling involves relatively large numbers of parameters, which are to a considerable extent constrained through the following considerations: 1) prior direct and independent measurements of forward and reverse rate constants by flow cytometry (12); 2) direct measurements of dissociation by the fluorescence method described in Fig. 2; and 3) the requirement that several experimental data sets be fit simultaneously (a) to association and dissociation kinetics, (b) to several ligand concentrations, and (c) in the presence and absence nucleotide. In general, unique fits were generated; in the cases in which individual parameters are not uniquely fit, they are indicated.

Results

Fluorescence quenching upon binding to the receptor. We have previously measured the quenching of pentapeptide fluorescence upon binding to the receptor by both cytometric and fluorometric methods. The intensity of bound ligand relative to free ligand is ~0.5 at pH 7.0 (12). The observed quenching of 5PEP fluorescence upon binding to its receptor allowed us to measure the time course of peptide binding with second time resolution (Fig. 2B). Dissociation can be induced by the addition of receptor antagonist (tbocFLFLF) and is observed as an increase in fluorescence intensity. The rate of dissociation is increased by two orders of magnitude upon the addition of saturating (10^{-4} M) GTP[S] (12). The association kinetics for ligand binding in the presence of saturating guanine nucleotide is fit to a single step (Fig. 2C, curve a). In contrast, ligand binding in the absence of guanine nucleotide is complex (Fig. 2C, curve b). The dissociation of L from cells exposed to saturating guanine nucleotide is fast and single step, while dissociation of L from cells that are not exposed to nucleotide is slow and complex (Fig. 2D). The sensitivity of binding to the presence of nucleotide, the complexity in the dissociation, and the slow approach to equilibration of the forward reaction in the absence of nucleotide all are consistent with a requirement for a ternary complex formalism for fitting the data (sides 1, 2, and 3 in contrast to sides 1 and 2 or 1 and 3).

To determine the rate constants for ligand-receptor interaction, we systematically examined ternary complex formation and dissociation as a function of ligand concentration (Fig. 3). Data points were collected within 1 sec after the addition of ligand and at 1-sec intervals. The time courses of binding from a single experiment repeated three times are shown in Fig. 3. The approach to equilibrium in the absence of nucleotide is slow (Fig. 3A), and dependent upon the ligand concentration. In the presence of saturating nucleotide (Fig. 3B), binding plateaus rapidly. Dissociation is induced by the addition of a large excess of ligand antagonist (tbocFLFLF). The behavior of ligand binding in permeabilized cells treated with N-ethylmaleimide was essentially identical to permeabilized cells exposed to saturating GTP[S].

To fit the binding data, we simultaneously fit the association

Downloaded from molpharm.aspetjournals.org at Thammasart University on December 2, 2012

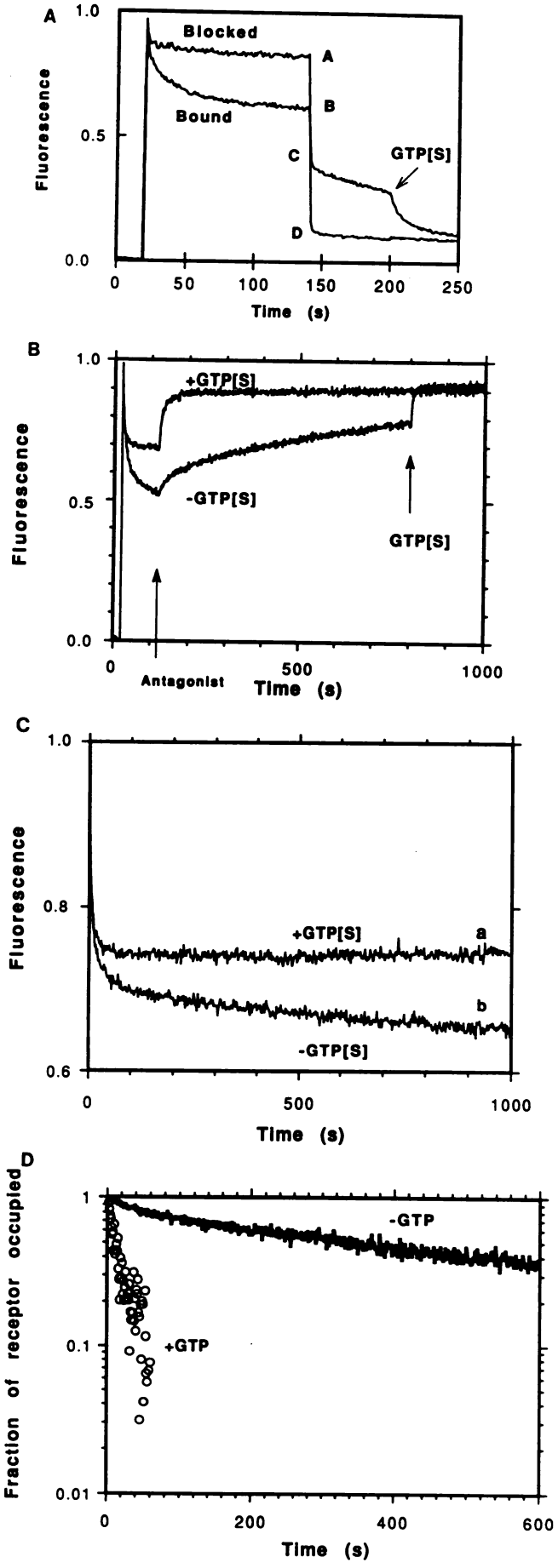

and dissociation experiments from three different ligand concentrations, both in the presence and absence of GTP[S] (Fig. 3). The experiments in which cells are exposed to saturating nucleotide are accounted for by a single-step process (Fig. 1, side 1). For the experiments in which guanine nucleotide is absent, we find that the association and dissociation behavior of ligand requires at least three sides of the complete cyclic ternary model (sides 1, 2, and 3 in Fig. 1). For the purpose of simplicity in this calculation, we take the concentration of G protein to be constant and in excess (see Discussion) and hence the concentration of G proteins enters only implicitly as a contribution to k_{+2}. With this model, the on-rate and the off-rate constants (k_{+1}, k_{-1}) of $\sim 2 \times 10^7$ M^{-1} sec^{-1} and ~ 0.1 sec^{-1}, respectively, are in close agreement with the values determined previously (with the same analysis) when the experiments were done by flow cytometry. Furthermore, the K_d calculated from the kinetic analysis (for the formation of LR in presence of nucleotide), ~5 nM (at 37°), compares well with the K_d of 2.6 nM (at RT) based on previous equilibrium measurements made cytometrically (12). Thus the fluorescent and cytometric approaches give similar data and appear to be equivalent.

The model used to fit the data in Fig. 3 (Fig. 1, sides 1, 2, and 3) allows for precoupling of receptors to G proteins but does not permit an independent kinetic analysis of side 4. (Allowing $k_{\pm 4}$ to be parameters gives no improvement in the fit). The variables include the total receptor concentration, the rate constants, and the fraction of precoupled receptors, RG. The values of the variables for simultaneous fits to all data sets shown in Fig. 3 (see Table 1) are: the total receptor concentration (0.90 nM in absence of guanine nucleotide, 0.80 nM in presence of guanine nucleotide); the fraction of RG (47% in absence of guanine nucleotide); the rates at which ligand binds to R or RG ($k_{+1-3} \sim 2.2 \times 10^7$ M^{-1} sec^{-1}) and dissociate from each ($k_{-1} \sim 1 \times 10^{-1}$ sec^{-1} for LR, $k_{-3} \sim 1 \times 10^{-3}$ sec^{-1} for LRG). The data require an interconversion step between LR and LRG. If the interconversion step is missing ($k_{\pm 2} = 0$), large systematic errors appear in the data. The parameters k_{+2} and k_{-2} were fit as 0.02 sec^{-1} and 1×10^{-4} sec^{-1}, respectively (see Discussion). In addition, there is a small fraction (~14%) of slowly dissociating sites even in the presence of saturating nucleotide (for the sake of simplicity, these sites are fit as a second class of receptors with $k_{on} = k_{+1}$ and $k_{off} = k_{-3}$).

Dissociation kinetics as a function of (GTP[S]). We

Fig. 2. Spectrofluorometric analysis of ligand-receptor interactions at 37° is shown as fluorescence versus time. A, Quantitation of free and bound ligand. To permeabilized cells (10^7/ml) was added 1 nM 5PEP (t = 20 sec), and antibody to fluorescein (t = 140 sec). The curve through *AD* traces a sample in which binding to the receptor is blocked by 10^{-5} M tbocFLFLF; the curve through *BC* represents binding to receptors; the addition of GTP(S) (t = 200 sec) reveals the proportion of receptors sensitive to nucleotide (i.e., LRG). B, Forward and reverse binding kinetics. In the presence (upper trace) or absence (lower trace) of 10^{-4} M GTP[S], 1 nM 5PEP was added to permeabilized cells (10^7/ml) at t = 20 sec to reveal forward kinetics of LRG and LR, respectively; 10^{-5} M tbocFLFLF was added at t = 120 sec to reveal reverse kinetics; 10^{-4} M GTP[S] was added to the lower curve at t = 800 sec to show that receptors remained sensitive to nucleotide. C, 5PEP (1 nM) was added to permeabilized cells (10^7/ml) at t = 0 sec. Shown is 1000-sec association kinetics to demonstrate forward binding reaction in the presence or absence of GTP(S). D, Permeabilized cells (10^7/ml) were preincubated with 1 nM 5PEP in presence or absence of 10^{-4} M GTP[S]. tbocFLFLF (10^{-5} M) was added (t = 0) to initiate dissociation of bound 5PEP. Six hundred-sec dissociation kinetics show single exponential dissociation in the presence of GTP(S) and complex dissociation in its absence.

MOL PHARM
MOLECULAR PHARMACOLOGY
aspet
Downloaded from molpharm.aspetjournals.org at Thammasart University on December 2, 2012

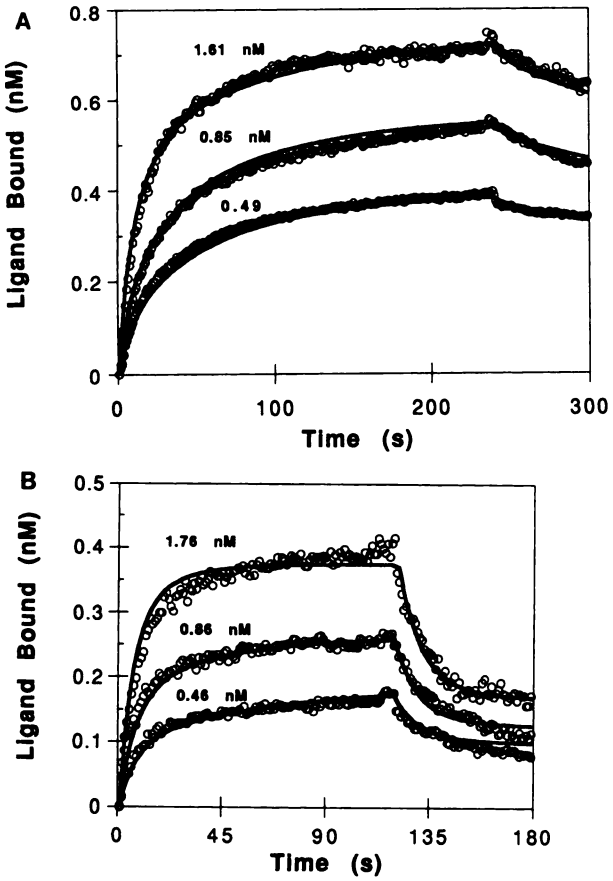

Fig. 3. Kinetic analysis of 5PEP binding and dissociation to permeabilized neutrophils at 37°. Data were obtained as in experiments illustrated in Fig. 2. The fluorescence intensity data were converted to concentration as described in Materials and Methods and are displayed after addition of 5PEP to cells (10^7cells/ml) at t = 0. Triplicate experiments for each ligand concentration were averaged in the (A) absence or (B) presence of GTP[S]. Dissociation was initiated by addition of a large excess of antagonist (tbocFLFLF) at t = 240 s (A) or at t = 120 sec (B). As described in the text, the data in (A) are modeled according to the scheme in Fig. 1, while the data in (B) are modeled as single-step reactions (represented by side 1, Fig. 1) with an allowance for a small fraction of slowly dissociating or nucleotide-insensitive receptors (treated as a second class of receptors with $k_{off} = k_{-3}$, side 3, Fig. 1). The final concentrations of 5PEP are shown on the figure. The computer fit fraction of nucleotide-insensitive receptors was 14%. This compares with a nominal value of ~15% measured at the time of permeabilization. The values for the rate constants are summarized in Table 1.

TABLE 1

Summary of the rate constants used to fit the data in Fig. 3

The parameters refer to the model in Fig. 1 and compared with previously published values by flow cytometry (12). * The calculations are relatively insensitive to values below 1×10^{-3} sec^{-1}.

	Fluorometry	Flow cytometry (12)
$k_{+1=3}$	2.2×10^7 M^{-1} sec^{-1}	2.7×10^7 M^{-1} sec^{-1}
k_{-1}	1.1×10^{-1} sec^{-1}	1.7×10^{-1} sec^{-1}
k_{+2}	2.1×10^{-2} sec^{-1}	$0.2–1 \times 10^{-2}$ sec^{-1}
k_{-2}	9.7×10^{-5} sec^{-1}*	*
k_{-3}	1.3×10^{-3} sec^{-1}	1.0×10^{-3} sec^{-1}
$RG(0)/R_T$	0.47	0.52

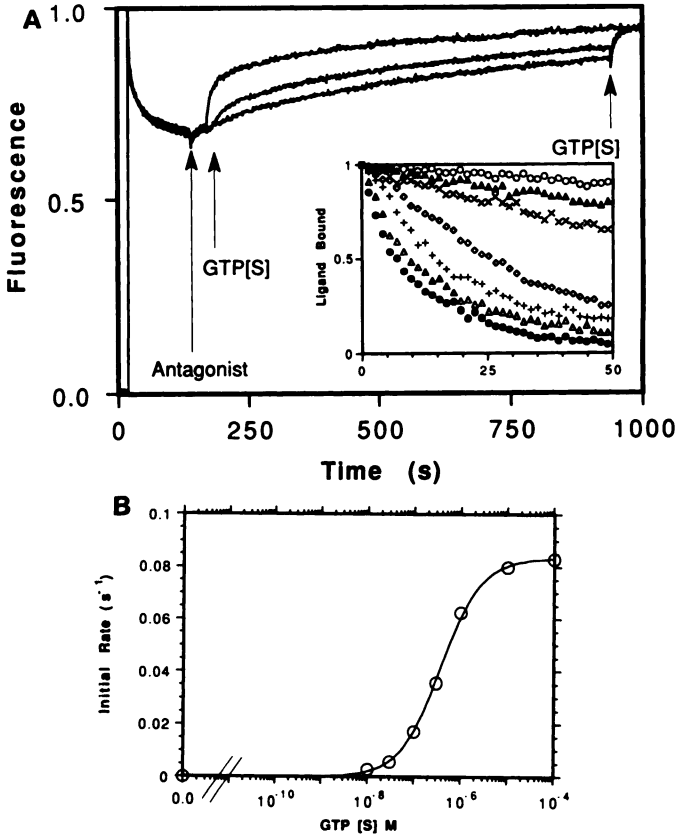

Fig. 4. Kinetics of ternary complex dissociation as a function of GTP[S] concentration. A, 5PEP (1 nM) was added at t = 20 sec to permeabilized cells (10^7/ml). At t = 120 sec (first arrow), tbocFLFLF (10^{-5} M) was added to compete with LR (at which time the residual receptors with bound ligand are LRG); GTP(S) was added at t = 180 sec (second arrow). (The data illustrated are for 0 (bottom curve), 10^{-7} M (middle curve), and 10^{-4} M (top curve) GTP[S]). At t = 930 sec, 10^{-4} M GTP [S] is added to the lower two curves. Inset: The dissociation of 5PEP from permeabilized neutrophils after the addition of indicated concentrations of GTP[S]. The data are normalized to reflect the disappearance of occupied receptors and shown with t = 0 as the time at which guanine nucleotide is added. The concentrations of GTP[S] are: 0 (○), 10^{-8} (▲), 3×10^{-8} (x), 10^{-7} (◇), 3×10^{-7} (+), 10^{-6} (△), and 10^{-4} (●) M. B, The data from (A) are plotted as the initial rate of nucleotide-induced dissociation of LRG upon the addition of GTP[S] versus nucleotide concentration. The initial rate of dissociation for nucleotide-induced LRG interconversion to LR is determined by subtracting the initial rate of dissociation of LRG for the case [GTP[S]] = 0 from each data set. (The rate of interconversion or nucleotide-induced dissociation in absence of GTP[S] is zero.) The solid curve represents a fit of the data to Eq. 3 as discussed in the text.

have examined the kinetics of ternary complex disassembly (Fig. 4). In these experiments, LRG is formed in the absence of guanine nucleotide, saturating antagonist is added to compete residual LR, then GTP[S] or other nucleotide is added (Fig. 4A). The rate of dissociation as a function of nucleotide concentration is shown in the inset and the calculated initial rates are shown in Fig. 4B. The rate is half-maximal near 10^{-7} M and saturates above 10^{-6} M. The potency of GTP is reduced by approximately one order of magnitude in concentration (not shown). The potency of GDP is reduced by ~3 orders of magnitude (not shown).

We have approached the data by considering that the steps involved in the dissociation of LR represent the interconversion of LRG to LR through an intermediate requiring the binding of nucleotide to LRG according to the scheme (19)[1] in Eq. 1.

[1] Published experiments (19) suggest that the delay between nucleotide binding and ternary complex disassembly is less than 500 msec; recent unpublished experiments limit the delay to < 100 msec. Because the delay is at least an order of magnitude slower than LR dissociation, the events appear to be essentially concerted on the time frame reported here.

MOL PHARM
MOLECULAR PHARMACOLOGY
aspet
Downloaded from molpharm.aspetjournals.org at Thammasart University on December 2, 2012

$$\mathrm{LRG} + \mathrm{GTP[S]} \overset{2}{\rightleftarrows} \mathrm{LRG\text{-}GTP[S]} \overset{3}{\longrightarrow} \mathrm{LR} + \mathrm{G^*\text{-}GTP[S]} \overset{4}{\longrightarrow} \mathrm{L} + \mathrm{R}$$
$$1 \downarrow$$
$$\mathrm{L} + \mathrm{RG}$$

where G^* is the activated form of the G protein and hence in the presence of GTP[S] is irreversibly formed. With GTP[S] concentrations above $\sim 10^{-6}$ M, the dissociation of ligand is essentially as rapid as it was from LR. This indicates that at high concentrations of guanine nucleotide, the nucleotide-dependent ligand dissociation from LRG is no slower than from preformed LR; that is, there is negligible delay (steps 2 and 3 are fast) between the time nucleotide binds and the time ternary complex decomposes into rapidly dissociating LR ($\sim 0.1\ \mathrm{sec}^{-1}$). Since step 3 is independent of the concentration of guanine nucleotide, the rate constant for step 3 must be $\gg 0.2\mathrm{s}^{-1}$.

We have simulated the net interconversion of LRG to LR as a single step (Eq. 2) in which the initial rate is $k_a \times [\mathrm{GTP(S)}]$. This method yields $k_a \sim 5 \times 10^5\ \mathrm{M}^{-1}\ \mathrm{sec}^{-1}$ (not shown).

$$\mathrm{LRG} + \mathrm{GTP[S]} \overset{k+a}{\longrightarrow} \mathrm{LR} + \mathrm{G^*\text{-}GTP[S]} \underset{k-b}{\overset{k+b}{\rightleftarrows}} \mathrm{L} + \mathrm{R}$$

We have also treated the data in Michaelis-Menten form using a quasi-steady state approximation (24) in which the initial rate (v) of dissociation is given by:

$$v = k_{+b}(\mathrm{LRG(0)})(\mathrm{GTP[S](0)})/(\mathrm{GTP[S](0)} + k_{+b}/k_{+a})$$

where LRG(0) and GTP(0) are the initial concentrations of LRG and GTP, respectively.

The maximum value for the initial rate is thus k_{+b} (LRG(0)) and the concentration of GTP[S] at $V_{max}/2$ is $(k_{-a} + k_{+b})/k_{+a}$. Because antagonist is added, $k_{-b} = 0$. The reverse step k_{-a} is neglected because GTP(S) is regarded as an irreversible activator.

Fitting the data in Fig. 4B to Eq. 3, we estimate that k_{+b} $\sim 0.1\ \mathrm{sec}^{-1}$ and that the value of $(k_{+b})/k_{+a} \sim 4 \times 10^{-7}$ M. Hence in this approach we conclude that the value for k_{+a} is $\sim 2.5 \times 10^5 \mathrm{M}^{-1}\ \mathrm{sec}^{-1}$ (i.e., the forward rate for step 2 (Eq. 1) is no less than $2.5 \times 10^5\ \mathrm{M}^{-1}\ \mathrm{sec}^{-1}$).

Distribution of LR and LRG in the presence of subsaturating (GTP[S]). As suggested above, there may be a fraction of R and G that is precoupled and GTP[S] is able to uncouple LRG. We therefore examined the effect of the availability of GTP[S] on the formation of ternary complex by varying GTP[S] before addition of ligand, as shown in Fig. 5. Intermediate concentrations of GTP[S] are observed to alter the extent of binding; that this altered binding reflects a change in distribution between LRG and LR can be seen in the dissociation behavior. As the concentration of GTP[S] increases, the behavior of the forward and reverse reactions increasingly takes on a character resembling LR. The data could be fit simply when the intermediate curves were represented as linear combinations of the curves obtained in the presence or absence of nucleotide (not shown) consistent with the idea of a redistribution between R and RG.

More rigorous fitting schemes were used to relate the behavior to ternary complex model. In the first scheme, the data for all the nucleotide concentrations were simultaneously fit to the model in Fig. 1 using the same variables described in modeling Fig. 3, but allowing the fraction of R and RG to be a function of the nucleotide concentration. When this was done, the following values for the rate constants were obtained: $k_{+1} \sim 2 \times 10^7\ \mathrm{M}^{-1}\ \mathrm{sec}^{-1}$, $k_{-1} \sim 0.1\ \mathrm{s}^{-1}$, $k_{-3} \sim 0.002\ \mathrm{sec}^{-1}$. If one uses small

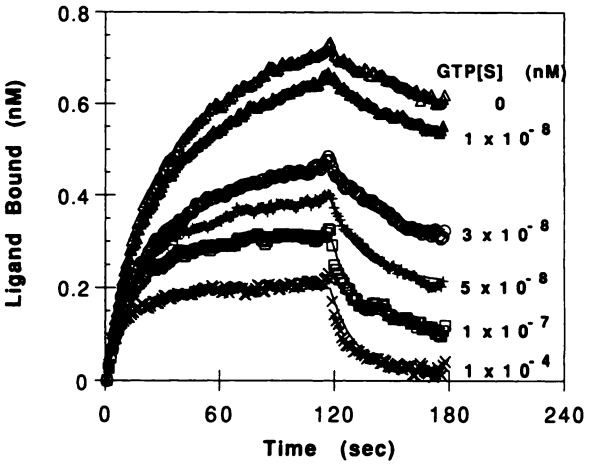

Fig. 5. Coexisting receptor states identified in the kinetics of 5PEP binding and dissociation to permeabilized neutrophils in presence of subsaturating concentrations of GTP[S]. Cells were preincubated with indicated concentrations of GTP[S] before the addition of peptide. Data display begins upon addition of pentapeptide to cells (10^7cells/ml) at t = 0. Dissociation was initiated by addition of a large excess of antagonist (10^{-5} M tbocFLFLF) at t = 120 sec. Duplicate determinations were averaged for each nucleotide concentration and fit as described in the text. The final concentration of the pentapeptide was 1.0 nM. The concentrations of GTP[S] are as indicated.

values for k_{+2} and k_{-2} ($<10^{-2}$ or $\sim 10^{-3}\ \mathrm{sec}^{-1}$, respectively), the data sets in Fig. 5 can be accounted for by allowing the fraction of receptor sites that are precoupled to vary, the values decreasing as the concentration of guanine nucleotide was increased. In this scheme, the fitted values for $[\mathrm{RG}]/\mathrm{R}_{\mathrm{Total}}$ at time $t = 0$ are 0.69, 0.61, 0.38, 0.23, 0.10, and 0.0 for GTP[S] concentrations of 0, 10^{-8}, 3×10^{-8}, 5×10^{-8}, 10^{-7}, and 10^{-4} M, respectively.

In the second scheme, we allowed k_{-2} (Fig. 1), the rate of nucleotide-dependent ternary complex disassembly (see below), to vary for each nucleotide concentration. This approach involves allowing LRG to break up after it forms at a rate dependent upon nucleotide concentration (a reasonable approach since k_{-2} implicitly contains the concentration of nucleotide). In this scheme the ratio of $\mathrm{RG}/\mathrm{R}_{\mathrm{Total}}$ (initial) is a parameter but is assumed to be the same for all GTP[S] concentrations. The errors in the fits to this model were only slightly greater than for scheme 1.

The first model allows nucleotide to affect side 4, redistributing R and RG in the absence of ligand. The second model allows nucleotide to affect side 2, redistributing LRG to LR. In an effort to distinguish between these models, we have performed additional experiments to determine whether preaddition of guanine nucleotide could redistribute RG. In these experiments (not shown), subsaturating GTP(S) (10^{-7}, 3×10^{-8}, or 10^{-8} M) was allowed to equilibrate for 0 sec, 10 sec, or 10 min with receptors before addition of ligand. These concentrations were low enough that their binding should have half-times between 30 sec and several minutes (see Fig. 4). No significant difference in the kinetics of ligand binding or dissociation was observed whether the nucleotide was added long before or just before ligand addition.

Discussion

The permeabilized neutrophil as model system for ternary complex interactions. The neutrophil formyl peptide receptor is a member of the family of seven transmembrane

MOL PHARM
MOLECULAR PHARMACOLOGY
aspet
Downloaded from molpharm.aspetjournals.org at Thammasart University on December 2, 2012

MOL PHARM

MOLECULAR PHARMACOLOGY

domain receptors and the neutrophil G protein, G_{i2}, is a member of the family of heterotrimeric nucleotide-binding proteins. Like the α- and β-adrenergic receptors and the muscarinic and dopamine receptors, the neutrophil receptors form a high affinity ternary complex (LRG) when nucleotide is absent and a low affinity LR complex when nucleotide is present (25, 26). As described previously, the digitonin permeabilized neutrophil retains these characteristics and appears to be a useful system for examining detailed interactions between receptors and G proteins.

The biochemistry of the ternary complex (25) assuming mobile receptors has the following elements: 1) in the absence of ligand, receptors and G proteins are dissociated; 2) G proteins normally exist as stable heterotrimers with bound GDP (we will use the notation G^+ and G^- to indicate occupied and empty G proteins); 3) upon ligand binding to the receptor, a short-lived quaternary complex forms (LRG^+); 4) the GDP is released from the quaternary complex after ligand binding to the receptor forming a high affinity ternary complex (LRG^-); 5) GTP binds to an empty ternary complex; and 6) GTP binding is followed by a concerted dissociation of the activated G protein from the receptor and a dissociation of the α-subunit of the G protein from the heterotrimer. Cell activation mediated through receptor-G protein interactions can occur on a subsecond time frame. The most notable example is the response of the rod outer segment to photons via rhodopsin (27). In the neutrophil, the generation of second messengers, such as Ca^{2+}, as well as oxidant responses, begins within a second or two after exposure to ligand (1). The experiments presented here address the kinetics of several of the steps of the model directly and contribute insight into several others.

Kinetic analysis of ternary complex assembly and disassembly. We reported previously a quantitative characterization of the formyl peptide receptor in the permeabilized human neutrophil using flow cytometry to discriminate free and bound ligand. In the absence of guanine nucleotide, dissociation of fluorescent formyl peptide from its receptor was slow (k_{off} ~10^{-3} sec^{-1}). When nucleotide was added at saturating concentration, a rapid release (k_{off} ~10^{-1} sec^{-1}) of ligand from 85% or more of the receptors was observed. These results are confirmed using the fluorescence method (Figs. 2 and 3). In the presence of guanine nucleotide, the receptors were detected as a population of sites with K_d ~2–5 nM. In the absence of guanine nucleotide, a major population of high affinity sites (K_d ~0.04 nM) coexists with a second site at equilibrium (12). Rapidly dissociating receptors with identical off-rates have also been detected when the cells were ribosylated with pertussis toxin or alkylated with *N*-ethylmaleimide (data not shown).[2] As in other systems and in previous biochemical measurements in intact neutrophils (6), the high affinity (slowly dissociating) binding was attributed to the ternary complex LRG and the low affinity (rapidly dissociating) binding to the binary complex LR.

The experiments in Fig. 3 compare the concentration dependence of ligand binding and dissociation with saturating GTP[S] or in the absence of guanine nucleotide. The data are similar to previous cytometric results, that is, the data can be fit with the same model (12) and validate the new methodology. In the presence of saturating guanine nucleotide or *N*-ethylmaleimide (not shown), the binding interaction behaves approximately as a single-step reversible reaction (Fig. 1, side 1) in which on- and off-rates are consistent with the equilibrium constant. The off-rate constants derived from simultaneously fitting the association and dissociation measurements (Fig. 3) are in agreement with direct measurement of the dissociation as analyzed by previous methods (6).

The experiments performed in the absence of nucleotide require complex models related to ternary complex formation (Fig. 1). In our analysis, we simultaneously fit the experiments performed in the presence of saturating nucleotide to the single-step model (using side 1 to represent the majority of the receptor and side 3 to account for the small fraction of nucleotide-insensitive receptors),[3] while the experiments performed in the absence of nucleotide are fit to more complex models. As can be seen from Fig. 1, we allow the rate constant (k_{+1}) for the binding of L to R and RG to be identical because the initial rates are experimentally identical (Figs. 2B, 2C, and 5). By fitting the two types of experiments (with and without nucleotide) simultaneously (to different models which have common parameters), we are able to restrict the parameters to values that are consistent with both types of experiments. We have used this approach to test a number of models with this data.

The *minimal* ternary complex analysis of the present spectrofluorometric data and the earlier cytometric data (12) requires three sides of the model (Fig. 1) when nucleotide is absent, as well as a large fraction of the receptors to be precoupled to G. This is the equivalent of allowing all four sides of the ternary complex model with the fourth side (representing the interconversion of R and RG) occuring at a slow rate. Single-site, independent two-site, and interconverting two-site (two sides) models are unable to account for all the features of the data (Fig. 2). Only more complex interconverting models incorporating receptor heterogeneity can fit the data. In the ternary complex analysis, this heterogeneity takes the form of "coupled" (represented as RG^- or RG^+) and "uncoupled" receptors (represented as R). In the formal ternary complex model, RG complexes are physically precoupled and the uncoupled receptors gain access to G proteins more slowly (with a half-time ~minutes) or not at all. The binding of ligand to coupled receptors (typically determined to be 40–50% of the total) occurs at a rate indistinguishable from the rate at which L binds to R. Computationally, one could not expect to distinguish unambiguously rapid coupling (half-times less than a second) from precoupling of receptors and G proteins. The fact that LR and LRG assemble with a very similar rate constant which approaches the diffusion limit for ligand binding to surfaces implies that ternary complex formation does not delay signal transduction. The stability of the ternary complex implies that nucleotide is absent from the complex (LRG^-), since adding nucleotide destabilizes the complex.

Simplifying assumptions in the analysis. 1) Because the number of parameters in the model in Fig. 1 is too large to permit unique fits to the data, we have previously evaluated increasingly complex versions of the ternary complex model, evaluating the improvements in fits by adding parameters from

[2] Treatment of permeabilized neutrophils with *N*-ethylmaleimide elevates the cellular autofluorescence to levels that hinder cytometric analysis yet do not interfere with the spectrofluorometric analysis.

[3] Preliminary experiments performed with new fluorescent formyl peptides revealed that a lower affinity ligand exhibited fewer nucleotide-insensitive receptors, a situation possibly related to the proposal of Samama *et al.* (28) of G protein-independent high affinity receptors.

Downloaded from molpharm.aspetjournals.org at Thammasart University on December 2, 2012

MOL PHARM

MOLECULAR PHARMACOLOGY

additional sides of the model, restricting parameters by making independent measurements of the individual sides or rates where possible, and fitting multiple data sets and experimental conditions where appropriate (12). Our analysis suggests that when using the ternary complex formalism, all four sides of the model (Fig. 1) are required, although we have been unable to obtain values for $k_{\pm 4}$ as the addition of these two parameters does not improve the quality of the fit. Rather we have included side 4 in the initial conditions (the concentrations of R and RG at $t = 0$; see part 3 below). The inclusion of all four sides of the model means that at least some fraction of receptors is able to find G protein in the absence of ligand.

2) The relative R and G stoichiometry may regulate access of receptors and G proteins. In several nonphotoreceptor systems (29–31) there appears to be a 10- to 100-fold excess of G proteins; nonetheless, it is common for receptors to have incomplete access to G proteins, some receptors forming ternary complex inefficiently. Since neutrophils may express 10,000–100,000 copies of 10 receptor types that couple to pertussis toxin-sensitive G proteins (32), the reduced access may involve competition or compartmentation of the components. Explicitly including the G protein concentration (Fig. 1, side 2) did not improve the fit to the data.

3) We include side 4 by allowing RG/R_{Total} at $t = 0$ to be a parameter. This is equivalent to assuming that the equilibration between R+G and RG is slow ($<10^{-2}$ sec^{-1})[4] or that there are two pools, one in which the equilibration is fast compared with ligand binding (side 1) and the other in which it is slow compared with side 3. We do not discriminate pools of G directly because the experiment in effect begins upon the addition of L. Allowing these rates to be included explicitly did not improve the fit. Analysis of side 4 equilibrium constant from the ratio of (RG) to $(R_{Total})(G)$ is precluded in the absence of knowledge of the effective (G).

4) The rate of ligand dissociation from LRG is $\sim 2 \times 10^{-3}$ sec^{-1}. We are unable to distinguish whether LRG disassembles through paths associated with sides 2 or 3 (i.e., according to k_{-2} or k_{-3}). Thus the value of k_{-2} is not uniquely determined and the values of k_{-2} and k_{-3} are correlated in this fitting scheme. Both parameters must be less than or equal to $\sim 10^{-3}$ sec^{-1}, and at least one of the parameters must be $\sim 10^{-3}$ sec^{-1}.

The kinetics of neutrophil signal transduction. The experiments of Figs. 4 and 5 suggest a time frame for ternary complex steps. While Figs. 3 and 5 require the rapid formation of LRG$^-$, Fig. 4 requires that once formed, the breakup of the ternary complex depends upon the availability of guanine nucleotide. The analysis of Fig. 4 shows that the rate of formation of LR from LRG increases with the nucleotide concentration and saturates at high nucleotide concentration. The rate of binding of GTP[S] is estimated to be no less that 2×10^5 M^{-1} sec^{-1}, a rate one to two orders of magnitude slower than the fastest rates of nucleotide binding to purified G protein (33, 34).[5]

The rate of interconversion from LRG to LR saturates at about 10^{-6} M GTP[S] or 10^{-5} M GTP (not shown). The overall rate of interconversion between LRG$^-$ and LR at physiological concentrations of GTP (35) is as fast as that shown here for saturating GTP[S]. Detection limits in these experiment require interconversion rates to be $\gg 0.2$ sec^{-1}, whereas stopped-flow experiments (19) imply interconversion rates to be $\gg 2$ sec^{-1}. With concerted G protein activation and ternary complex disassembly, G protein activation in the intact cell is predicted to be occurring in a time frame of no greater than a few hundred msec after the binding of the ligand to the receptor. Therefore, the data presented here indicate that the *k*inetics of formation and decomposition of ternary complex for a full agonist are appropriate to transduction in the subsecond time frame in the neutrophil. It is possible that activation by partial agonists may be delayed by less efficient ternary complex dynamics (36).

The rapid formation of ternary complex (LRG$^-$) could in principle arise in several ways. The conventional explanation is that LR complexation with G is diffusion-limited and is followed by the rapid release of GDP to form a stable LRG$^-$. The analysis of Fig. 3 and Fay *et al.* (12) provide two alternative routes which should be considered: 1) precoupled RG$^+$ complexes lose GDP rapidly upon ligand binding; or 2) precoupled RG$^-$ complexes bind ligand directly. Because G proteins are isolated with bound GDP, empty G proteins are found in cells only if endogenous GDP is released by ligand and receptor. Because GTP[S] activates heterotrimeric G protein in broken cells including the neutrophil, it is possible that RG$^-$ complexes are activated directly in the absence of ligand. We attempted to obtain evidence for such a path by making nucleotide binding the rate-limiting step in ternary complex disassembly (not shown), then assaying LR/LRG distribution. Since the distribution between LR and LRG was apparently insensitive to the length of incubation with GTP[S], we have not obtained new evidence for the interaction of GTP[S] with RG in the absence of ligand. These experiments have proven to be technically difficult because of the relatively slow rates of ligand binding achieved with the reagent concentrations used here.

Comparison between cytometric and spectrofluorometric approaches to ternary complex analysis. Since cellular transduction events such as ligand binding, receptor-G protein coupling and uncoupling, and second messenger generation can all occur in a subsecond time frame, there is a clear need for real-time assays of ligand binding. We have previously used a commercial flow cytometer with a sample transit time of ~5 sec where the ability to examine forward and reverse processes was limited by the difficulty of on-line sample manipulation (12). The spectrofluorometric assay considerably improves the time resolution and ease of introduction of reagents into the sample, permitting continuous observation to examine the dynamics of ternary complex formation and breakup in real-time. On the other hand, the spectrofluorometric approach requires that a significant fraction of the ligand present must be bound, and the signal to background fluorescence ratio deteriorates as excess ligand increases. Direct binding measurements in the presence of nucleotide require ~nM R (i.e., $\sim 10^7$ neutrophils/ml) and the range of ligand concentration is limited. The cytometric assay is optimally performed at cell densities of $\sim 10^6$ neutrophils/ml. Since the cytometric assay intrinsically discriminates bound ligand in a sea of free ligand, it permits a much greater range of ligand concentration.

[4] Simulations reveal only subtle differences in ligand-binding kinetics when equilibration rates between R and RG exceed 10^{-2} sec^{-1}.

[5] It is worth noting that: 1) the highest rates of nucleotide binding to purified G proteins are approximately two orders of magnitude less than the diffusion limit; and 2) the binding of small molecules to membrane receptors is reduced one to two orders of magnitude from the diffusion limit. Our rate constant represents a minimal value for nucleotide binding to a membrane-bound G protein. The value would be increased by reverse reactions in Eq. 2 and by the presence of other nucleotide-binding sites in the preparation.

aspet

Downloaded from molpharm.aspetjournals.org at Thammasart University on December 2, 2012

While the spectrofluorometer presently provides better time resolution and is suited to stopped-flow analysis (19), recent hardware and software developments suggest that it should ultimately be possible to have comparable intrinsic time resolution in the two methods. Because the spectrofluorometric and cytometric assays require cell concentrations that differ by an order of magnitude, a direct comparison of raw ligand binding data is not possible. By showing that the fluorometric data (Fig. 3) are best fit to the same model (with similar parameters) as the previous cytometric data (12), we have demonstrated the equivalency of the two methods.

In summary, we have introduced a real-time assay of ligand-receptor interactions suitable for the formyl peptide receptor. We have shown that the method provides results essentially identical to an earlier cytometric method but offers improved time resolution. Finally, we have applied the method to several dynamic aspects of the ternary complex model which have not been evaluated previously.

Acknowledgments

We would like to thank Dr. Richard Freer for a gift of the fluorescent formyl pentapeptide and Dr. Richard Neubig for helpful discussions concerning the analysis of nucleotide-dependent ternary complex disassembly.

References

1. Wymann, M. P, V. Tscharner, D. A. Deranleau, & M. Baggioloini. The onset of the respiratory burst in human neutrophils. *J. Biol. Chem.* **262**:12048–12053 (1987).
2. Smigel, M. D., E. M. Ross, & A. G. Gillman. Role of the b-adrenergic receptor in the regulation of adenylate cyclase. in *Cell Membranes*, Vol. 2. Plenum, New York, 247–294 (1984).
3. Spain, J. W., & C. J. Coscia. Multiple Interconvertible affinity states for the opioid agonist-receptor complex. *J. Biol. Chem.* **262**:8948–8951 (1987).
4. Lynch, C. J., S. J. Taylor, J. A. Smith, & J. H. Exton. Formation of the high-affinity agonist state of the α_1 adrenergic receptor at cold temperature does not require a G protein. *FEBS Lett* **229**:54–58 (1988).
5. Sklar, L. A., G. M. Bokoch, D Button, & J. E. Smolen. Regulation of ligand-receptor dynamics by guanyl nucleotides: rapidly interconverting states for the neutrophil formyl peptide receptor. *J. Biol. Chem.* **262**:135–139 (1987).
6. Sklar, L. A., H. Mueller, G. Omann, & Z. Oades. Three states for the formyl peptide receptor on the intact cell. *J. Biol. Chem.* **264**:8483–8486 (1989).
7. Tardif, M., L. Mery, L. Brouchon, & F. Boulay. Agonist-dependent phophorylation of N-formylpeptide and activation peptide from the fifth component of C (C5a) chemoattractant receptors in differentiated HL60 cells. *J. Immunol.* **150**:3534–3545 (1993).
8. Neubig, R. R., R. D. Gantzos, & R. S. Brasier. Agonist and antagonist binding to a_2-adrenergic receptors in purified membranes from human platelets. *Mol. Pharmacol.* **28**:475–486 (1985).
9. Kim, M., & R. R. Neubig. Parallel inactivation of a_2-adrenergic agonist binding and Ni by alkaline treatment. *FEBS Lett.* **192**:321–325 (1985).
10. De Lean, A., J. M. Stadel, & R. J. Lefkowitz. A ternary complex model explains the agonist-specific binding properties of the adenylate cyclase coupled beta-adrenergic receptor. *J. Biol. Chem.* **255**:7108–7117 (1980).
11. Lee, T. W. T., M. J. Sole, & J. W. Wells. Assessment of a ternary complex model for the binding of agonists to neurohumoral receptors. *Biochemistry* **25**:7009–7020 (1986).
12. Fay, S. P., R. G. Posner, W. N. Swann, & L. A. Sklar. Real-time analysis of the assembly of ligand, receptor and G-protein by quantitative fluorescence flow cytometry. *Biochemistry* **30**:5066–5075 (1991).
13. Neubig, R. R., R. D. Gantzos, & W. J. Thomsen. Mechanism of agonist and antagonist binding to a_2 adrenergic receptors: evidence for a precoupled receptor-guanine nucleotide protein complex. *Biochemistry* **27**:2374–2384 (1988).
14. Thompsen, W. J., J. A. Jacquez, & R. R. Neubig. Inhibition of adenylate cyclase is mediated by the high affinity conformation of the a_2-adrenergic receptor. *Mol. Pharmacol.* **34**:814–822 (1988).
15. Fay, S. P., M. D. Domalewski, & L. A. Sklar. Evidence for protonation of ligand in the binding pocket of the formyl peptide receptor. *Biochemistry* **32**:1627–1631 (1993).
16. Sklar, L. A., S. P. Fay, B. E. Seligmann, R. J. Freer, N. Muthukumaraswamy, & H. Mueller. Fluorescence analysis of the size of a binding pocket of a peptide receptor at natural abundance. *Biochemistry* **29**:313–316 (1990).
17. Sklar, L. A. Real time spectroscopic analysis of ligand-receptor dynamics. *Annu. Rev. Biophys. Biophys. Chem.* **16**:479–506 (1987).
18. Sklar, L. A., D. A. Finney, Z. G. Oades, A. J. Jesaitis, R. G. Painter, & C. G. Cochrane. Dynamics of ligand receptor interactions. Real-time cytometric and fluorimetric assays of association, dissociation and internalization of an N-formyl peptide and its receptors on human neutrophils *J. Biol. Chem.* **259**:5661–5669 (1984).
19. Neubig, R. R., & L. A. Sklar. Subsecond modulation of formyl-peptide-linked G proteins by GTPgS in permeabilized neutrophils. *Mol. Pharmacol.* **43**:734–740 (1993).
20. Tolley, J. O., G. M. Omann, & A. J. Jesaitis. A high-yield, high purity elutriation method for preparing human granulocytes demonstrating enhanced experimental lifetimes. *J. Leukocyte Biol.* **42**:43–50 (1987).
21. Smolen, J. E., S. J. Stoehr,, A. E. Traynor, & L. A. Sklar. The kinetics of secretion from permeabilized human neutrophils: release of elastase and correlations with other granule constituents and right angle light scatter. *J. Leukocyte Biol.* **41**:8–13 (1987).
22. Muthukumaraswamy, N., & R. J. Freer. Synthesis of chemotactic peptides. *Methods Enzymol.* **162**:3860–3874 (1987).
23. Levison, S. A., A. N. Hicks, A. J. Portman, & W. B. Dandliker. Fluorescence polarization and intensity kinetic studies of antifluorescein antibody obtained at different stages of the immune response. *Biochemistry* **14**:3778–3786 (1975).
24. Segal, L. A. On the validity of the steady-state assumption of enzyme kinetics. *Bull. Math. Biol.* **50**:579–793 (1988).
25. Gilman, A. G. G proteins: transducers of receptor-generated signals. *Annu. Rev. Biochem.* **56**:615–649 (1987).
26. Dohlman, H. G., J. Thorner, M. G. Caron, & R. J. Lefkowitz. Model systems for the study of seven-transmembrane-segment receptors. *Annu. Rev. Biochem.* **60**:653–688 (1991).
27. Chabre, M., & P. Deterre. Transducin, rhodopsin, and 3′,5′-cyclic GMP phosphodiesterase: typical G protein mediated transduction system, in *G proteins* (R. Iyengar & L. Birnbaumer, eds.). Academic Press, New York, 215 (1990).
28. Samama, P., S. Cotecchia, T. Costa, & R. J. Lefkowitz. A mutation-induced activated state of the b_2 adrenergic receptor. Extending the ternary complex model. *J. Biol. Chem.* **268**:4625–4636 (1993).
29. Asano, T., R. Morishita, M. Sano, & K. Kato. The GTP-binding proteins, G_0 and G_{i2}, of neural cloned cells and their changes during differentiation. *J. Neurochem.* **53**:1195–1198 (1989).
30. Mueller, H., R. Weingarten, L. A. Ransnas, G. M. Bokoch, & L. A. Sklar. Differential amplification of antagonistic receptor pathways in neutrophils. *J. Biol. Chem.* **266**:12939–12943 (1991).
31. Ransnas, L. A., & P. Insel. Quantitation of the guanine nucleotide binding regulatory protein G_s in S49 cell membranes using antipeptide antibodies to a_s. *J. Biol. Chem.* **263**:9482–9485 (1988).
32. Sklar, L. A. Ligand-receptor dynamics and signal amplification in the neutrophil. *Adv. Immunol.* **39**:95–143 (1986).
33. Ferguson, K. M., T. Higashijima, M. D. Smigel, & A. F. Gilman. The influence of bound GDP on the kinetics of nucleotide binding to G proteins. *J. Biol. Chem.* **261**:7393–7399 (1986).
34. Higashijima, T., K. M. Ferguson, M. D. Smigel, & A. F. Gilman. The effect of GTP and Mg^{+2} on the GTPase activity and the fluorescent properties of G_o. *J. Biol. Chem.* **262**:757–761(1987).
35. Sklar, L. A., H. Mueller, W. N. Swann, C. Comstock, G. M. Omann, & G. M. Bokoch. Dynamics of interaction among ligand, receptor, and G protein. *ACS Symp. Ser.* **383**:52–69 (1989).
36. Tota, M. R., & M. I. Shimerlik. Partial agonist effects on the interaction between the atrial muscarinic receptor and the inhibitory guanine nucleotide binding protein in a reconstituted system. *Mol. Pharmacol.* **37**:996–1004 (1990).

Send reprint requests to: Dr. Larry Sklar, Department of Cytometry, University of New Mexico, School of Medicine, Albuquerque, NM 87131.

MOL PHARM
MOLECULAR PHARMACOLOGY
aspet
Downloaded from molpharm.aspetjournals.org at Thammasart University on December 2, 2012